Available online at www.sciencedirect.com
SCIENCE DIRECT®
Vacuum 77 (2005) 371–376
VACUUM
SURFACE ENGINEERING, SURFACE INSTRUMENTATION & VACUUM TECHNOLOGY
www.elsevier.com/locate/vacuum

Comparison of back-foil SXRF and EPMA for the elemental characterization of thin coatings

E.S. Valamontes[a,*], J.C. Statharas[b]

[a]Department of Electronics, Technological and Educational Institute of Athens, 12210 Aegaleo, Greece
[b]Department of Mechanical Engineering, Technological and Educational Institute of Chalkis, 34400 Psahna, Euboea, Greece

Received 20 May 2004; accepted 18 November 2004

Abstract

Back-foil scanning X-ray microfluorescence (SXRF), developed in a scanning electron microscope and applied for the analysis of very thin coatings is compared with electron probe X-ray microanalysis (EPMA). Both experimental results and Monte-Carlo calculations are used in this respect. The signal to background ratio as a function of the primary electron beam energy and angle of incidence, and for different film thicknesses is obtained for both techniques and a comparative study of sensitivity is made. Back-foil SXRF used in optimized experimental conditions, is found to be more sensitive than EPMA, especially in the case of very thin overlayers. The resolving power of back-foil SXRF is also calculated for the anode used by Monte-Carlo simulations.

Keywords: X-ray microanalysis; X-ray microfluorescence; Thin films

1. Introduction

X-ray fluorescence (XRF) and electron probe X-ray microanalysis (EPMA) are two analytical techniques with quite different characteristics. EPMA uses electron excitation in an electron microscope while XRF uses an X-ray excitation source, which offers several advantages over the electron excitation: (a) more sensitive than energy dispersive EPMA, (b) possibility of analyzing insulators without depositing a conducting layer on top of them, (c) possibility of nondestructive analysis of beam-sensitive biological samples where these are not sensitive to the level of X-radiation involved. On the other hand, EPMA offers the advantage of a much better lateral resolution, in the μm range, which allows imaging of the analyzed element of the sample.

Several attempts have been made to use the electron source of the electron microscope in order to obtain an X-ray source inside the microscope. Middleman and Geller [1] fixed an attachment

*Corresponding author. Tel.: +301 5385305, fax: +301 6511723.
E-mail address: vala@ee.teiath.gr (E.S. Valamontes).

0042-207X/$ - see front matter © 2004 Elsevier Ltd. All rights reserved.
doi:10.1016/j.vacuum.2004.11.002

with a 25-μm-thick molybdenum foil, used as an X-ray source, generated by a 30 keV electron beam. Analogous attachments were proposed by Linnemann and Reimer [2], Wendt [3,4] and Weiss [5], all of them mounting their transmission X-ray sources far from the specimen to be analyzed. Slightly different, but always with the X-ray source far from the specimen were the attachments proposed by Eckert (both reflection [6] and transmission [7,8]) and Pozsgai (transmission mode, but with the analyzed specimen in a closed space, protected from unwanted X-rays [9]). Other works, dealing with analogous SEM attachments, are nicely described in a review article by Pozsgai [10].

A somewhat different solution was proposed by Cazaux [11] and implemented first in a surface analysis instrument [12] and later in a scanning electron microscope [13]. It consists of a thin film anode in close contact with a thin film sample. The X-rays created within the anode under electron bombardment ionize the atoms of the sample. The corresponding SEM attachment [13] is illustrated in Fig. 1. Compared to all the other proposed solutions, this experimental arrangement offers the ultimate resolution, which is in the μm range when the anode is sufficiently thin (of the order of the electron range). In this paper, this last solution is used (back-foil scanning X-ray microfluorescence(SXRF)) and the sensitivity of the technique for the analysis of very thin overlayers, where EPMA reaches its detection limits, is examined. Both experimental results and Monte-Carlo simulations are used in this respect. Direct comparison with EPMA is also made. The radial distribution of the obtained fluorescence signal is also calculated by Monte-Carlo simulations.

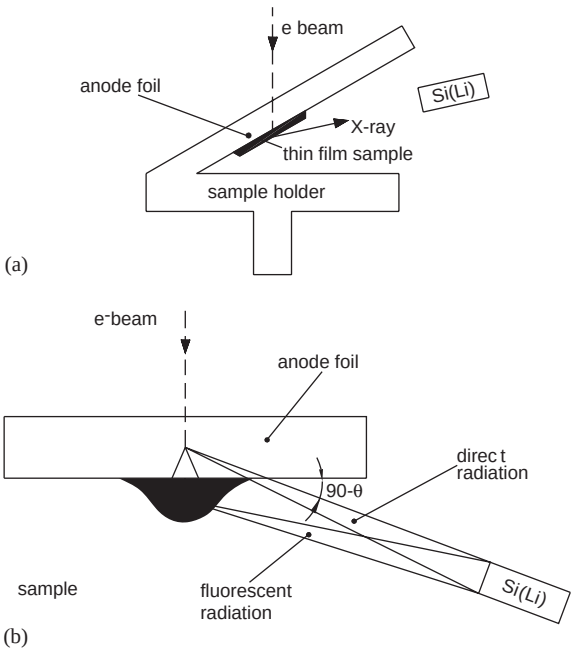

Fig. 1. (a) Experimental setup used for back-foil XRF, the anode is composed of a nickel foil, 5 μm thick or of a silicon foil, 20 μm thick. (b) Illustration of the trajectories of primary and fluorescence X-rays in back-foil XRF. The background is reduced by absorption of the continuous radiation, created by the electron beam, within the anode.

2. Experimental setup

The experimental setup of Fig. 1a was used for back-foil XRF. The anode was composed of a nickel foil, 5 μm thick (case a) or a silicon foil, 20 μm thick (case b). The anode was chosen to be sufficiently thick so that primary beam electrons were prevented from reaching the Ti film (case a) or the Al film (case b) on the back side of the anode. On the other hand, a limited thickness is necessary in order to minimize self absorption of the generated X-rays. Titanium films (case a) or Al films (case b) of different thicknesses were deposited on one side by electron beam evaporation in high vacuum (10^{-3} Pa). A Si(Li) detector and an EDAX system for quantitative analysis were used for X-ray signal acquisition. The X-ray signal, integrated under the peak and the integrated background, also under the peak and in the same energy window, were used. Standard EPMA, using the same experimental conditions of beam current and electron beam focusing was applied to the same samples.

3. Monte-Carlo calculations

The basic computational model for the calculation of electron trajectories was described in detail

elsewhere [14]. It is based on the following assumptions:

- elastic scattering is described by a screened Rutherford cross-section
- angle deviation is considered to be only due to elastic scattering, this is a good approximation, as inelastic scattering occurs through very small angles
- between two scattering points, electrons are considered to lose energy continuously.

The energy loss is described by the Bethe equation [15] for energies $E > 6.4\,\mathrm{J}$, where J is the mean ionization potential. For lower energies, the Rao–Sahib and Wittry's [16] expression is used.

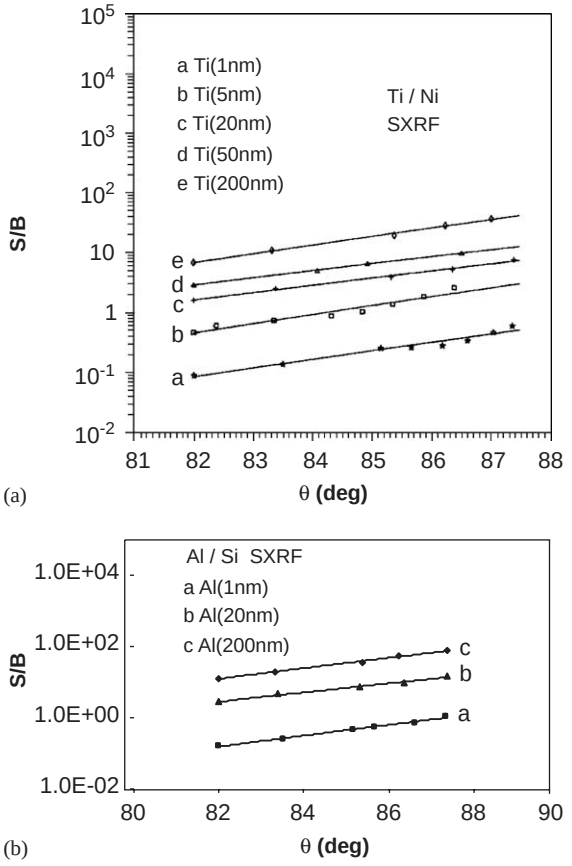

Fig. 2. (a) Experimental values of the signal to background ratio (S/B) in the case of back-foil XRF for Ti/Ni system and different film thicknesses as a function of the detection angle θ. (b) Experimental values of the signal to background ratio (S/B) in the case of back-foil XRF for Al/Si system and different film thicknesses as a function of the detection angle θ.

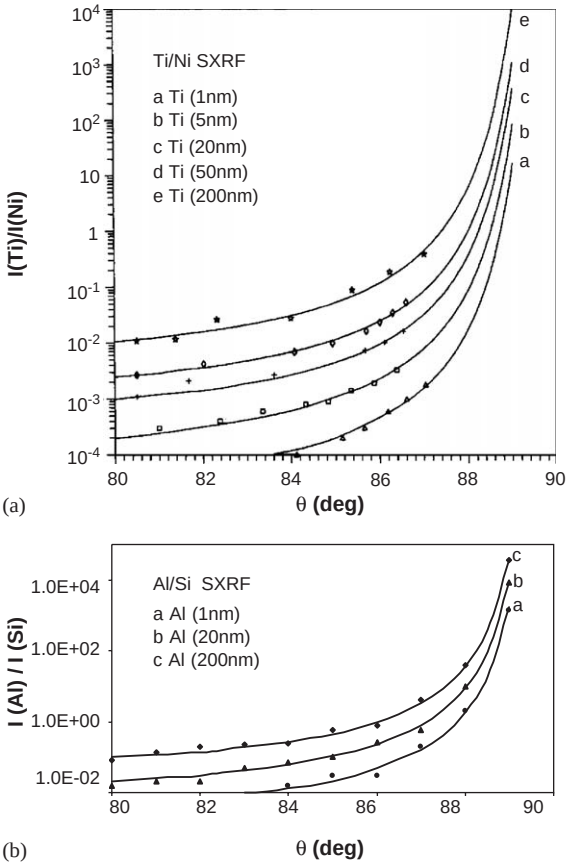

Fig. 3. (a) Ratio of the Ti X-ray signal from the film to the Ni X-ray signal from the anode. Points correspond to experimental results and full lines to Monte-Carlo calculations. (b) Ratio of the Al X-ray signal from the film to the Si X-ray signal from the anode. Points correspond to experimental results and full lines to Monte-Carlo calculations.

- Each step length for elastic scattering is considered to be constant and equal to 1/100 of the total electron range (plural scattering model). The total length of the electron trajectory within the sample is taken to be the Bethe range. With this approximation, the calculation time is reduced significantly while little error is introduced. In order to evaluate the X-ray signal induced by electrons, each step is divided into smaller steps. At each small step, the energy and

position of the electron is known, so the probability for X-ray generation is given by the corresponding cross-section.

The X-ray emission is considered to be isotropic, two random numbers are used for the direction of X-ray emission. Some of these X-rays enter into the film after possible absorption within the anode.

The XRF signal is calculated by dividing the film into 10 layers and considering the probability that the primary X-rays entering the layer are absorbed by the layer on their way out of the film. Absorption correction of the fluorescent X-ray signal created within the film is also considered. The absorption coefficients used, are taken from the X-ray cross-section compilation by the Kaman Science Corporation [17].

4. Results and discussion

Fig. 1b illustrates the trajectory of the direct and fluorescence X-rays in back-foil XRF. The background is reduced by absorption of the continuous radiation, created by the electron beam, within the anode.

Figs. 2 (a and b) indicates the experimental results of the signal to background ratio (S/B) in the case of back-foil XRF for different film thicknesses as a function of the detection angle θ. The acquisition time of the whole spectrum was equal to 600 s. When the angle is increased, the S/B ratio is improved, due to further reduction of the background caused in turn by greater absorption of continuous radiation within the anodes and an increase of the analyzed film areas.

Fig. 3a shows the ratio of the analyzed Ti X-ray signal from the film to the Ni signal from the anode and Fig. 3b the ratio of the analyzed Al X-ray signal from the film to the Si signal from the anode. Points correspond to experimental results and full lines to Monte-Carlo calculations. Good agreement is observed between experiment and calculations. The Ti signal (case a) and the Al signal (case b) from the films are increased with respect to the signals from the anodes as the detection angle θ is increased. This is due to an increase in the analyzed areas and to the absorption. The absorption of the Ni and Si X-ray lines

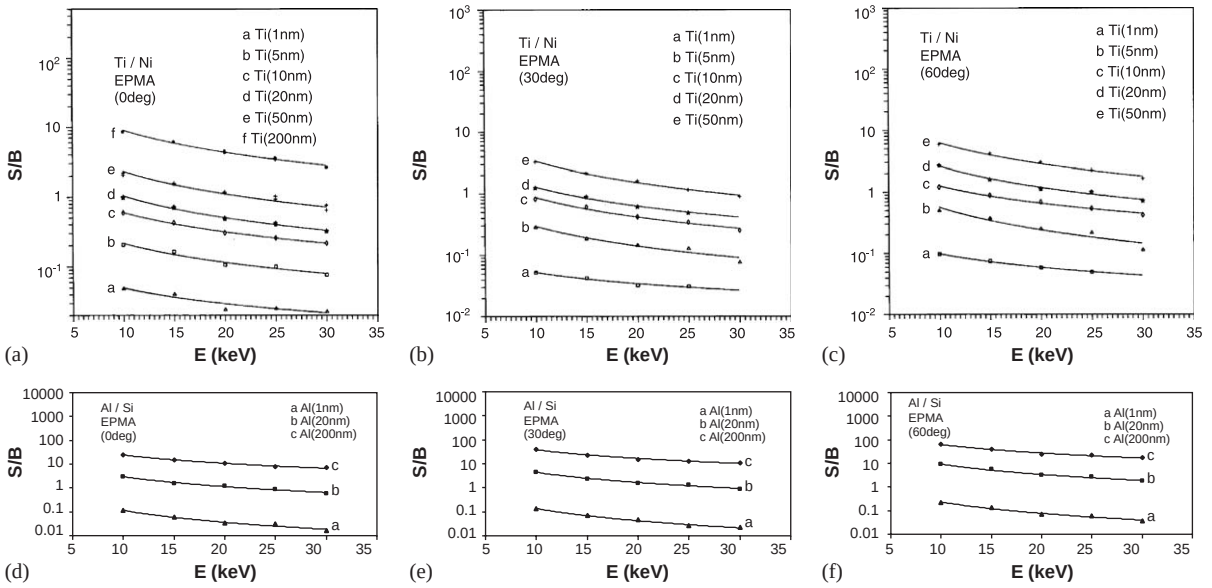

Fig. 4. (a–c) Experimental values (EPMA) of the signal to background ratio (S/B) for Ti/Ni system and three different angles of incidence (0°, 30°, 60°). (d–f) Experimental values (EPMA) of the signal to background ratio (S/B) for Al/Si system and three different angles of incidence (0°, 30°, 60°).

from anodes is greater than the absorption of Ti and Al XRF signals from the films with the increase of θ angle.

EPMA was performed on the same samples for comparison. The signal from a thin film in EPMA is improved at low primary beam energies and high angles of incidence. Figs. 4a–f illustrate experimental results of the signal to background ratio (S/B) for Ti/Ni and Al/Si systems and three different angles of incidence. If we compare Fig. 2a with Figs. 4a–c and Fig. 2b with Figs. 4d–f we see that in back-foil XRF the signal to background ratio is two or three times higher than in EPMA. The same acquisition time was used for both EPMA and back-foil XRF spectra (600 s). But we have to note that the reduced background in the case of back-foil XRF permits an increase in the acquisition time and improved sensitivity. Indeed the minimum detectable concentration (or thickness) is calculated by considering the Rose criterion, according to which a signal is detectable if the corresponding peak is at least three times the standard deviation of the background. By taking that into account the minimum detectable concentration X_m of an element A in a matrix may be expressed as:

$$X_m = \frac{3}{I_S}\sqrt{\frac{I_{BG}}{t}},$$

where I_S is the signal from a standard containing only element A and I_{BG} is the signal under the background. From the above expression it is obvious that the minimum detectable concentration is reduced if I_{BG} is smaller and the acquisition time is increased. In the case of back-foil XRF the reduced background gives the possibility to increase the measuring time so that the sensitivity of the technique is considerably improved compared to that of EPMA.

The lateral distributions of the total X-ray signals from the films in back-foil XRF is given in Figs. 5a and b for primary beam energy of 30 keV. These distributions are approximately Gaussians. By applying the Rayleigh criterion as in Ref. [18], the resolving power of the technique, defined as the minimum distance between two points for which the X-ray signals are resolved, is

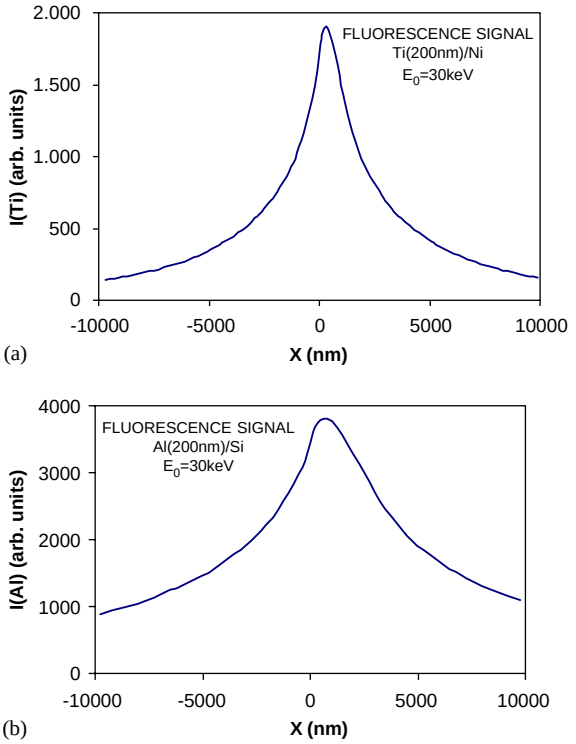

Fig. 5. (a) The lateral distribution of the total X-ray signal from a Ti (200 nm) film /Ni in back-foil XRF for a primary beam energy of 30 keV. (b) The lateral distribution of the total X-ray signal from an Al (200 nm) film /Si in back-foil XRF for a primary beam energy of 30 keV.

calculated. Values of 3.7 μm (case a) and of 9.2 μm (case b) are found for the anode thicknesses and primary beam energy used. These resolving powers are by some orders of magnitude better than in standard XRF.

5. Conclusion

Back-foil scanning XRF and EPMA are both applied to the analysis of very thin films. The sensitivity of back-foil XRF is better than that of EPMA in the case of very small film thicknesses (up to a few tens of nm). The obtained experimental results are verified by Monte-Carlo calculations. The resolving power of back-foil XRF is of the order of some micrometers. This is much better than the resolving power in conventional

XRF and of the same order of magnitude as in EPMA.

Acknowledgment

This work is co-funded by 75% from E.E. and 25% from the Greek Government under the framework of the Education and initial Vocational Training Program—Archimedes (project TEI of Athens 2.2–23).

References

[1] Middleman LM, Geller JD. Scanning electron microscopy, Part I. Chicago: IITRI; 1976. p. 171–177.
[2] Linnemann B, Reimer L. Scanning 1998;1:109.
[3] Wendt M. Patentschrift DD-WP 1978;139:304.
[4] Wendt M, Krajewski T. In: Proceedings of 5 Tagung Microsonde, Physikalische der DDR, Leipzig, 1981. p. 125–9.
[5] Weiss RM. Beitr. Elektronenmikroskop. Direktabl. Oberfi 1979;2:209.
[6] Eckert R. Scanning electron microscopy, vol. IV. O'Hare, Chicago: SEM inc. AMF; 1983. p. 1535–1545.
[7] W. Plannet, Leaflet Rontgenbox, Plano, Marburg, 1983.
[8] Eckert R. Scanning 1986;8:232.
[9] Pozsgai I. Inst Phys Conf Ser 1985;78:201.
[10] Pozsgai I. X-ray Spectrometry 1991;20:215.
[11] Cazaux J. Rev Phys Appl 1975;10:263.
[12] Mouze D, Thomas X, Cazaux J. In: Brown JD, Packwood RH, editors. Proceedings of 11th international Congress on X-ray optics and microanalysis. London, Canada, 1986. pp. 63–66.
[13] Valamontes E, Nassiopoulos AG. In: Proceedings of III Balkan Congress on electron microscopy. Athens, 1989. pp. 267–268.
[14] Nassiopoulos AG, Valamontes E. Surf Interf Anal 1990;15:405.
[15] Bethe H. Ann Phys (Leipzig) 1930;5:325.
[16] Rao-Sahib TS, Wittry DB. J Appl Phys 1974;45:5060.
[17] X-ray cross-section compilations from 0.1 keV to 1 MeV, Kaman Science Corporation, Colorado Springs, CO.
[18] Valamontes E, Nassiopoulos AG, Glezos N. Surf Interf Anal 1992;19:419.